Training in cortically-blind fields confers patient-specific benefit against retinal thinning after occipital stroke

Berkeley K. Fahrenthold PhD[1], Matthew R. Cavanaugh PhD[1], Madhura Tamhankar MD[2], Byron L. Lam MD[3], Steven E. Feldon MD[1], Brent A. Johnson[4] and Krystel R. Huxlin PhD[1]

[1]Flaum Eye Institute and Center for Visual Science, University of Rochester, Rochester, NY, USA.
[2]Scheie Eye Institute, University of Pennsylvania, Philadelphia, PA, USA.
[3]Bascom Palmer Eye Institute, University of Miami, Miami, FL, USA.
[4]Department of Biostatistics and Computational Biology, University of Rochester, Rochester, NY, USA

Corresponding author: Krystel R. Huxlin, PhD, Flaum Eye Institute, University of Rochester Medical Center, 601 Elmwood Avenue, Box 314, Rochester, NY, 14642, USA. Email: khuxlin@ur.rochester.edu, phone: 1-585-275-5495.

Total word count: 3,500 or fewer (currently ~4,000)

Funding Information: This work was supported by NIH funding (R01 EY027314 to KRH, as well as T32 EY007125 and P30 EY001319 to the Center for Visual Science), and by an Unrestricted Grant from the Research to Prevent Blindness (RPB) Foundation to the Flaum Eye Institute. The HIS clinical trial was funded by a Center of Emerging and Innovative Science for Empire State Development (project no. 1730C004), a Center of Excellence (project no. 1689bC2) and EnVision Solutions LLC. The sponsors and funding organizations had no role in the design or conduct of this research.

23 **Commercial Relationships Disclosures:** KRH is an inventor on US Patent No. 7,549,743. The

24 remaining authors have no competing interests.

Abstract

Purpose: Damage to the adult primary visual cortex (V1) causes vision loss in the contralateral hemifield, initiating a process of trans-synaptic retrograde degeneration (TRD). Here, we examined retinal correlates of TRD using a new metric to account for global changes in inner retinal thickness, and asked if perceptual training in the intact or blind field impacts its progression.

Methods: We performed a meta-analysis of optical coherence tomography (OCT) data in 48 participants with unilateral V1 stroke and homonymous visual defects, who completed clinical trial NCT03350919. After measuring the thickness of the macular ganglion cell and inner plexiform layers (GCL-IPL), and the peripapillary retinal nerve fiber layer (RNFL), we computed individual laterality indices (LI) at baseline and after ~6 months of daily motion discrimination training in the intact- or blind-field. Increasingly positive LI denoted greater layer thinning in retinal regions affected *versus* unaffected by the cortical damage.

Results: Pre-training, the affected GCL-IPL and RNFL were thinner than their unaffected counterparts, generating LI values positively correlated with time since stroke. Participants trained in their intact-field exhibited increased $LI_{GCL-IPL}$. Those trained in their blind-field had no significant change in $LI_{GCL-IPL}$. LI_{RNFL} did not change in either group.

Conclusions: Relative shrinkage of the affected *versus* unaffected macular GCL-IPL can be reliably measured at an individual level and increases with time post-V1 stroke. Relative thinning progressed during intact-field training, but appeared to be halted by training within the blind field, suggesting a potentially neuroprotective effect of this simple behavioral intervention.

47

Non-standard Abbreviations and Acronyms:

CB – Cortical Blindness

OCT – Optical Coherence Tomography

LI – Laterality Index

dLGN – dorsal lateral geniculate nucleus

GCL-IPL – Ganglion Cell Layer-Inner Plexiform Layer

RGC – Retinal Ganglion Cell

HIS - Hemianopia Intervention Study

HVF – Humphrey Visual Field

OU – Oculus Uterque (both eyes)

OS – Oculus Sinister (left eye)

OD – Oculus Dextrus (right eye)

SEM – Standard Error Mean

PMD – Perimetric Mean Deviation

ST_{BF} – Mean Sensitivity of Blind Field

TRD – Trans-synaptic Retrograde Degeneration

Introduction

Cortical blindness (CB) following unilateral damage to the primary visual cortex (V1) or its immediate afferents presents as a homonymous, contra-lesional visual field defect. Although partial recovery can occur spontaneously in the first few months after damage[1–4], there are no widely-accepted, validated treatments for the resulting visual defect[5]. Standard of care remains "no intervention", although occasionally, patients are prescribed compensatory (e.g. saccadic) training or substitution (e.g. prism lenses) therapies[6–9]. Research also continues to show that visual perceptual training can partially restore vision in CB, measurable by both clinical perimetry and psychophysical tests of visual performance[10–21].

The importance of developing some form of restorative therapy for CB is further highlighted by burgeoning evidence that once patients reach the chronic stage of >6 months post-stroke, visual field defects do not remain completely stable, as was initially thought[22]. Instead there appears to be progressive worsening of the perimetrically-defined blind field (BF) without intervention[11,19,22,23]. The most plausible explanation for such deterioration of the BF over time is TRD, which involves the progressive shrinkage and even die-back of neurons in the early visual pathways[24–31]. In humans, structural MRI analyses have shown that the optic tract ipsilateral to occipital cortex damage is often reduced in size[25,29,30,32–35], as are the thicknesses of the ganglion cell and nerve fiber layers in corresponding regions of the retina in each eye[24,28–32,34,36–45].

Retinal ganglion cells (RGCs) are responsible for pre-processing and ferrying visual information to the rest of the visual system. As such, their loss or dysfunction could significantly threaten the potential to recover visual functions in participants with V1 damage. Specifically,

retinal neurons in the therapeutically-targetable retino-geniculate-striate pathways susceptible to trans-synaptic retrograde degeneration (TRD) after occipital stroke. Isolating specific consequences of TRD in retinal regions known to synapse with V1-lesion-projecting neurons in the lateral geniculate nucleus is crucial to better understand the relationship between TRD and visual retraining. Approaches to re-train the visual deficit have been shown to confer perimetrically-computed improvements to CB visual fields[16,46]. However, most literature has focused on benefits to visual perception resulting from visual retraining, with limited knowledge of the effects of training on anatomical substrates of vision[16,46]. If visual training strengthens existing circuitry or recruits neuronal neighbors, similar to rehabilitation for motor stroke[47–49], this could potentially impact retinal cells that provide input to residual visual pathways. As such, the present study asked two questions: 1) what is the extent and time-course of relative thinning in affected *versus* unaffected inner retinal layers in humans with unilateral occipital strokes, and 2) does the stimulation afforded by visual training impact the progression of inner retinal thinning in such stroke patients? To answer these questions, we performed a meta-analysis of optical coherence tomography (OCT) data collected as part of a recently-completed, multicenter, randomized, double-masked, clinical trial titled the "Hemianopia Intervention Study" (HIS; ClinicalTrials.gov identifier, NCT03350919). The HIS clinical trial design and results have been published in detail[50], but in brief, the trial involved 2 pre-training clinic visits to establish eligibility and measure baseline parameters, a 6-months at-home phase during which training was administered to either the intact field (IF) or BF, and 1 post-training clinic visit to evaluate the effect of training. The primary outcome measure for the HIS clinical trial was change in the 24-2 Humphrey perimetric mean deviation (PMD) from

baseline, with significant improvements reported for people trained in their BF, and not those trained in their IF.[50] However, the trial also performed OCT imaging and collected measurements of GCL-IPL and RNFL thicknesses in the affected and unaffected retina of each eye in each participant at each time-point. This rich data set provided us a unique opportunity to both measure the extent of TRD in this patient cohort, and analyze the impact of two different of visual training interventions on TRD progression.

Methods

Participants

The HIS trial (NCT03350919) recruited 48 CB participants (see **Table 1** for demographics) at 3 US academic medical centers: 20 at the University of Rochester's Flaum Eye Institute, 18 at the University of Pennsylvania's Scheie Eye Institute and 8 at the University of Miami's Bascom Palmer Eye Institute. All procedures were approved by the Western Institutional Review Board (WIRB#1181904), adhered to the tenets of the Declaration of Helsinki and all participants gave written, informed consent.

Participants were between 21 and 75 years of age, with an MRI-confirmed occipital lesion resulting in unilateral homonymous hemianopia. Additionally, their lesions had to have occurred after the age of 18 and a minimum of 90 days prior to screening. Participants were also required to reliably fixate with both eyes during psychophysical testing and clinical Humphrey perimetry, with fixation losses, false-negative, and false-positive rates during perimetry of <20%. Participants were excluded from the study if they presented with any ocular or neurologic disease that would interfere with training. Concurrent use of any other form of visual therapy, or of medications that would affect training were additional exclusion criteria.

HIS clinical trial design and training intervention

As mentioned earlier, the HIS clinical trial[50] involved 2 pre-training clinic visits, a 6-month at-home training phase and 1 post-training clinic visit. While the primary outcome measure was change in the 24-2 Humphrey PMD from baseline to 6 months post-training, OCT data were also collected at each study visit, followed by computerized psychophysical testing focused on

instructing participants to correctly perform the training task. Once enrolled, participants were randomized to 2 training arms: intact field (IF) or blind field (BF) training - in a 1:1 ratio, using a permuted block design stratified by site. Participants randomized to these training groups did not differ in age (BF-trained: 56±12 years, range 32-72 years; IF-trained: 61±9 years, range 45-74 years; unpaired t-test p= 0.0990, CI_{95}=-11.83 to 1.057) or time since stroke (BF-trained: 41±82 months, range 3-373 months; IF-trained: 43±72 months, range 3-338 months; unpaired t-test p=0.9096, CI_{95}=-50.37 to 44.98).

The training intervention was a 2-alternative, forced-choice (2AFC), direction discrimination task using random dot stimuli presented either inside the BF or at a corresponding location in the IF (**Table 1, Supplementary Materials, Supplementary Fig. S1**). During the home training segment, two participants withdrew and their data are not included herein. The two cohorts trained for a comparable number of days (unpaired t-test p=0.3598, CI_{95}=-43.82 to 16.27; BF-trained: 101±46 days; IF-trained: 115±51 days).

During pre-training, in-clinic assessment, participants received instructions and underwent baseline testing with this task within their intact and blind hemifields, with fixation enforced binocularly using an Eyelink Duo Mobile eye-tracker (SR Research, Mississauga, Ontario, Canada). Training locations were selected at sites where performance first dropped to chance (50% correct) after a 1° lateral shift along the x-axis from the intact into the BF. Using the location where performance first drops to chance as a starting point affords proximity to intact circuitry, enhancing the possibility that training may recruit perilesional V1[51], and/or induce plasticity and re-integration of residual, damaged circuitry. IF-training locations were selected to be mirror-symmetric to those chosen for training in the BF. CB participants were

then sent home to train and were asked to perform 300 trials of the 2AFC task once daily for a minimum of 5 days per week, at their assigned, training location. Participants trained at a single location at a time, either in the IF or BF. Once performance improved sufficiently (at least 10 sessions at a threshold <25˚ with a standard deviation of less than 5˚), the location was moved 1° laterally away from the vertical meridian. Participant performance as a result of these interventions has been published[50] and will not be repeated here in detail.

Humphrey visual field testing and analysis

Each participant's visual deficit was quantified through Humphrey visual field (HVF) perimetry, which was performed twice in both eyes during each study visit. The University of Rochester and the University of Pennsylvania used a Humphrey Field Analyzer II-i, and the University of Miami used a Humphrey Field Analyzer 3 (Zeiss Humphrey Systems, Atlanta, GA), with all sites using a 24-2 testing pattern. A white, size III stimulus was presented on a background with a luminance of 11.3 cd/m^2 and thresholds were calculated with the Swedish Interactive Threshold Algorithm (SITA-standard). Participants' visual acuity was corrected to 20/20 for testing, and fixation was controlled using the gaze/blind spot automatic settings. The first test was excluded in both eyes to account for potential learning effects. If the second field set was not deemed reliable or could not be completed, the first set was used instead. Participants who did not have complete, reliable pre- and post-training visual fields were excluded from the present HVF analyses(n=5); an additional two participants failed to complete training and were also removed from our analysis. Two metrics were derived from HVF tests: the perimetric mean deviation (MD) and the average luminance detection sensitivity across the entire blind

183 hemifield of vision. The MD is calculated by the perimeter using an internal, weighted variance
184 from age-defined normal population values, to estimate the amount of vision lost across the
185 measured visual field. In the present study, sensitivity thresholds from the blind hemifield (ST_{BF})
186 were additionally averaged in each eye to capture deficit-specific changes. We then took the
187 monocular MD and ST_{BF} and averaged them to generate a binocular (OU) version of each
188 metric, for pre- and post-training comparisons, in order to compare with binocularly-computed
189 OCT laterality indices.
190
191 **Optical coherence tomography (OCT) procedures and analysis**
192 Retinal OCT was performed using Cirrus HD machines (Carl Zeiss Meditech) at each study site
193 before and after training. A 512 × 128 Mac Cube scan was used to examine the ganglion cell
194 and inner plexiform layers (GCL-IPL) around the fovea, and 200 × 200 optic nerve cube scans
195 were used to examine the retinal nerve fiber layer (RNFL). Scans were excluded if they failed to
196 meet signal strength ≥7 in each eye.
197 OCT analyses performed as part of the HIS clinical trial[50] differed from those performed
198 here in several ways. First, they involved group-level comparisons of GCL-IPL and RNFL
199 thickness changes pre- to post-training across affected and unaffected retinal regions,
200 separated by blind field sector and for each eye independently. Here, for the GCL-IPL, we
201 combined the 2 nasal sectors together, and the two temporal sectors together. Furthermore,
202 after reviewing OCT raw data, we excluded 3 HIS participants due to retinal folding or epiretinal
203 membrane/RNFL detachment severe enough to impact layer thickness measurements. In

204 remaining participants, we then computed a laterality index (LI) to account for individual,
205 baseline thickness variances using the following formula:

$$\boldsymbol{Laterality\ Index} = \frac{(\boldsymbol{Intact} - \boldsymbol{Blind})}{(\boldsymbol{Intact} + \boldsymbol{Blind})}$$

206 LI was computed for the GCL-IPL using the 2 nasal and 2 temporal sector values of both eyes,
207 excluding superior and inferior sectors that overlapped the vertical meridian (**Fig. 1A**). The nasal
208 and temporal macular segments of each eye corresponding to the blind or intact hemifield
209 were then averaged together according to each participant-specific deficit. For example, a right-
210 sided visual deficit (left-sided occipital lesion) is represented in the nasal sectors of the right eye
211 and the temporal sectors of the left eye (see example in **Fig. 1A**).

212 Computing a laterality for the RNFL regions impacted by the deficit attempted to
213 account for the crossed and uncrossed fibers in corresponding peripapillary sections[52] (**Fig. 2A**).
214 Superior and inferior peripapillary regions comprised of uncrossed fibers, and nasal
215 peripapillary regions comprised of crossed fibers represent intact or blind hemifields. For
216 example, the same right-sided visual deficit area described above was represented by the
217 superior and inferior RNFL sectors of the left eye as well as the nasal RNFL sector of the right
218 eye (**Fig. 2A**).

219

220 **Statistical Analyses**

221 Paired t-tests were used to assess within-subject differences. For independent sample
222 comparisons, unpaired t-tests were used when contrasting 2 groups. If standard deviations
223 were not the same in each group, Welch's correction was used. Linear regressions were used to

model the relationship between explanatory variables and dependent outcomes, with r values and 95% confidence intervals (CI_{95}) for rho provided, and significance estimated using a t-test.

Results

Baseline retinal layer thicknesses – effects of time since stroke

Prior to intervention, GCL-IPL thicknesses corresponding to the blind or intact hemifields were significantly different from each other, with the affected hemiretina's GCL-IPL being thinner than the unaffected hemiretina's (**Fig.1B**). We then computed LI to factor out possible global retinal phenomena (e.g., aging-related, metabolic, etc.) in order to better isolate lesion-specific degeneration in retinal regions corresponding to perimetrically-defined visual deficits. The $LI_{GCL-IPL}$ was positive, averaging 0.056 ± 0.06, with a range of -0.068 to 0.29. An LI of 0 would indicate no relative thinning of the lesion-projecting compared to the non-lesion projecting part of the retina, while positive LI values denote thinning in retinal areas representing the blind hemifield relative to those representing the intact hemifield. Importantly, the $LI_{GCL-IPL}$ was positively correlated with time since stroke (**Fig. 1C**), with greater thinning of the affected hemiretina GCL-IPL in participants imaged beyond 12 months post-stroke compared to those imaged prior to this timepoint (**Fig. S2A**).

A similar pattern of results was obtained for the peripapillary RNFL, which was thinner for segments carrying RGC axons representing the visual field defect compared to those carrying predominantly intact field fibers (**Fig.2B**). As a result, LI_{RNFL} averaged 0.019 ± 0.04, ranging from -0.10 to 0.11. Moreover, just like $LI_{GCL-IPL}$, LI_{RNFL} was positively correlated with time since stroke (**Fig. 2C**), with relative thinning most pronounced beyond 12 months post-lesion (**Fig. S2B**). Overall, these data show clear GCL-IPL and RNFL thinning in regions of the retina carrying either RGC somata, dendrites and/or axons representing blind regions of the visual

248 field. They also show greater thinning at later than earlier timepoints, especially >12 months
249 after occipital stroke.

250

251 **Effect of visual training on GC complex thickness**

252 We next asked whether visual training altered signs of TRD at the level of the retina. Here, we
253 analyzed CB patients who completed 6 months of visual training as part of the HIS clinical
254 trial[50]. As previously reported, global direction discrimination training in the perimetrically-
255 defined BF of CB patients elicits improvements not only on the trained task, but also on
256 binocular (OU) Humphrey perimetry[11,50]. Consistent with this observation, participants trained
257 in their BF exhibited a systematic improvement in OU MD (**Fig.3A**). To ascertain if the change in
258 MD was driven by the blind hemifield (*versus* improved ability to perform Humphrey perimetry
259 across the entire test area), we also computed OU ST_{BF} change for the blind hemifield. OU ST_{BF}
260 improved significantly following BF training (**Fig. 3B**), contrasting with a lack of significant
261 changes - for both OU MD and ST_{BF} - in the IF-trained cohort (**Fig. 3D, E**). Notably, a strong
262 correlation exists between MD and ST_{BF} in both cohorts, pre- and post-training (**Fig. 3C, F**).

263 Having established a subtle but differential effect of training on perimetry between the
264 two cohorts, we then asked if - and to what degree - the two types of intervention impacted
265 retinal thinning. For $LI_{GCL-IPL}$, there was a significant overall increase pre- to post-training across
266 all participants (**Fig. 4A**). However, no detectable changes occurred pre- to post-training overall
267 in LI_{RNFL} (**Fig. 4B**). Separating the two interventions, $LI_{GCL-IPL}$ was significantly larger post-training
268 in those who trained in their intact field (**Fig.5A**), but not in BF-trained participants (**Fig.5B**).
269 Furthermore, in the IF training group, raw GCL-IPL thicknesses were significantly lower in the

post-training affected hemiretina (**Fig. 5C**). Post-training affected GCL-IPL thicknesses also significantly changed from pre-training in the BF training group (**Fig. 5D**). Additionally, a significant difference in magnitude of change in the affected relative to unaffected hemiretinas was present in IF trained participants and, critically, no such difference was found in BF trained participants (**Fig. 5E**). However, we fail to reject the null hypothesis that the pre-post differences of the affected hemiretinas differ by training type (**Fig. 5E**).

When assessing the impact of training on the RNFL, no significant change in LI_{RNFL} was found in either group pre- to post-training (**Fig. 6A, B**). Similarly, no significant pre-post training differences were observed in either training cohort for raw RNFL thickness (**Fig. 6C, D**). Additionally, when assessing pre-post change, no significant differences were seen between or within training groups (**Fig. 6E**).

Consistent with these findings, changes in ST_{BF} and $LI_{GCL\text{-}IPL}$ were directly [and inversely] correlated in those trained in their blind hemifield (**Fig. 7A**), but not in those trained in their IF (**Fig. 7B**). No significant correlations were observed between changes in ST_{BF} and LI_{RNFL} in either training cohort (**Fig. 7C, D**).

Discussion

The present study asked – for the first time – whether visual stimulation provided by perceptual training alters the progression of retinal ganglion cell layer complex thinning after stroke damage to the occipital cortex in adult humans. First, we confirmed prior reports of relative thinning in the affected *versus* unaffected retinas' GCL-IPL and RNFL after unilateral V1 damage[28,29,31,32,34,36,39,41,53] using non-invasive OCT imaging. Second, the spread of post-stroke times at participant enrollment allowed us to define a time-course for this thinning. Finally, we now provide evidence that a simple behavioral intervention slows or blocks the progression of relative GCL-IPL thinning whereas comparable stimulation of the intact hemifield of vision fails to do so.

Occipital damage causes variable, progressive shrinkage of the GC complex

Our observations showed that the largest, positive deviations from 0 in $LI_{GCL\text{-}IPL}$ and LI_{RNFL} occurred beyond 12 months post-stroke. While some deviation in $LI_{GCL\text{-}IPL}$ (but not LI_{RNFL}) was also observed in our earliest participants, there was considerable inter-individual variability which precluded a significance analysis in the present cohort. Large deviations of LI values from 0 were previously observed for optic tract volumes using structural magnetic resonance imaging, starting from ~6 months post stroke, albeit also with large inter-individual variability[35]. This time-course differential makes some sense if one considers that the optic tract contains the distal portions of RGC axons, right before they synapse in the dorsal lateral geniculate nucleus. These distal axons, being closer to the V1 lesion site, might exhibit earlier signs of target loss and degeneration than the cell bodies and dendritic arbors of the parent cells in the

retina, but once again, a larger sample size earlier post-stroke would be needed to make this determination from a statistically-valid standpoint.

As stated earlier, a positive LI reflects a relative thinning of the lesion-projecting *vs.* intact-hemisphere-projecting portions of the macular GCL-IPL. This relative thinning could be attributable to shrinking of the RGC soma, cell death, and/or changes in cell branching; similarly, relative thinning in the RNFL could result from RGC axonal loss or shrinkage or both[24,28,29,32,34,37,40,53–55]. Though past studies show that RGCs are ultimately lost over time after occipital damage[28,29,31,55,56], there is also evidence that RGCs change size based on metabolic activity or the beginning stages of apoptosis[57,58]. As such, slowing or even reversing retinal thinning may be possible if intervention occurs prior to significant cell death.

Importantly, both the GCL-IPL and RNFL were previously reported to thin with increasing age in humans[59], a fact confirmed in the present data set, and is likely related to cell loss and/or shrinkage (**Fig. S3**). However, it is important to note that by computing and tracking changes in LI rather than raw layer thicknesses, we were able to dissociate the impact of the occipital stroke and subsequent training interventions, from this natural trend.

Visual training blocks the progression of *relative* GC complex thinning

In spite of initial retinal ganglion cell complex thinning at baseline, participants who trained in their BF for 6 months showed improvements in binocular performance metrics derived from Humphrey perimetry and seemed to avoid the increase in $LI_{GCL\text{-}IPL}$ that occurred in participants randomized to train in their IF. While GCL-IPL thickness decreased in both groups, the change in GCL-IPL thickness of the affected relative to the unaffected hemiretina was only significant in

the IF-trained participants. Coupled with a failure to reject the null hypothesis in pre- to post-training differences of $LI_{GCL-IPL}$ in the BF-trained group, this suggests a subtle but significant effect of training location on GCL-IPL thinning within a given patient, which is lost when comparing effects across individuals. The inherent variability in OCT layer thickness in small cohorts makes it difficult to compare groups directly. This is further complicated by variability introduced due to time-dependent TRD. In the future, increasing the sample size to increase sensitivity is crucial to better understanding the anatomical underpinnings of visual retraining. This is a difficult endeavor with two critical limitations 1) CB participants with lesions limited to the occipital cortex are rare and challenging to recruit and 2) once recruited, CB participants require time-intensive testing and evaluation. Alleviating these limitations would require expansion of collaborating facilities and personnel, as well as relaxing inclusion and exclusion recruitment criteria, leading to a more heterogenous patient population. However, despite current limitations these within-group comparisons provide novel insights into training-dependent changes within the early visual pathway.

These surprising observations suggest first that OCT imaging and our derived LI metric is a sensitive biomarker for assessing the impact of training in post-stroke CB patients. Just as importantly, it also suggests that an intervention which locally stimulates RGCs in a retinal area deprived of several key central targets may benefit the structural integrity of these residual cells. In turn, this may increase the likelihood that these neurons are retained long-term in the residual visual circuitry, perhaps providing the neural substrates of training-induced recovery of visual functions seen deeper into the visual deficit[51]. Conversely, training within the intact field locally stimulates circuits that are not directly affected by V1 damage-mediated TRD[26,29,43].

353 Though V1 areas of both hemispheres representing visual information along the vertical
354 meridian are connected via callosal axonal projections[60], notable due to the training locations
355 of these participants, these interhemispheric connections do not appear to provide enough
356 benefit to anterior portion of the visual pathway to be observable at the level of the retina.

357 So, what could underlie the stabilization of $LI_{GCL-IPL}$ in BF-trained participants? As
358 mentioned earlier, damaged RGCs undergo changes in their dendritic arbors in the IPL[61,62] and
359 in supporting cells, such as muller glia[57,58,63], which span the entire thickness of the retina.
360 Training in the BF could increase the energy demands of stimulated RGCs, and by consequence,
361 of surrounding supporting cells, in turn causing structural changes manifested as a cell-size
362 increase and/or shrinkage prevention[36,57]. Changes in surviving RGCs are of course likely
363 occurring in tandem with RGC loss due to retrograde degeneration – a phenomenon on which
364 visual training's effects are unknown.

365 An important question emerging from the present results is whether the stabilization of
366 the $LI_{GCL-IPL}$ persists after BF training stops. If this phenomenon relies on increased retinal
367 activity due to training, it is possible that physiological mechanisms of TRD will eventually
368 overcome the benefits gained once training ceases. However, it is also possible that if
369 participants incorporate their regained visual abilities into everyday usage, they could maintain
370 them and sustain their associated circuits.

371 Finally, we saw no significant changes in LI_{RNFL} or RNFL thickness in either training
372 cohort, although several factors likely limited our ability to detect such changes with OCT,
373 including the anatomical complexities of the RNFL in different peripapillary zones, the very
374 small volume of the RNFL overall, our relatively small sample size and inter-subject variability.

375 Future studies using larger sample sizes, more detailed analyses and better imaging resolution
376 will be required to rigorously elucidate the impact of training on the RNFL.
377
378 **Conclusion**
379 In conclusion, the present work investigated the impact of a visual training intervention
380 administered either inside the blind or intact field of occipital stroke patients on the
381 progression of TRD at the level of the inner retina. We found that relative thinning in the GCL-
382 IPL and RNFL mirrored a distinct time-course post-stroke previously reported in the literature.
383 Training for ~6 months with a motion discrimination task inside the blind hemifield appeared to
384 block the progression of relative thinning in the ganglion cell complex. In contrast, this relative
385 thinning proceeded unabated when training was administered to the intact field of vision. Our
386 results provide the first evidence of a greater structural benefit in the retina for a behavioral
387 intervention that stimulates circuitry impacted by V1 damage, over one that stimulates the
388 intact circuitry.
389
390
391

392 **Disclosures:** Berkeley K. Fahrenthold, None; Matthew R. Cavanaugh, None; Madhura

393 Tamhankar, None; Byron L. Lam, None; Steven E. Feldon, None; Brent A. Johnson, None;

394 Krystel R. Huxlin, inventor on US Patent No. 7,549,743 (P)

395

References

1. Gray CS, French JM, Bates D, Cartlidge NE, Venables GS, James OF. Recovery of visual fields in acute stroke: homonymous hemianopia associated with adverse prognosis. *Age Ageing*. 1989;18:419–421.

2. Lin S, George BZ, Wilson-Holt NJ. Perimetric demonstration of spontaneous visual field recovery following occipital lobe haemorrhage. *BMJ Case Rep.* 2013;2013.

3. Zhang X, Kedar S, Lynn MJ, Newman NJ, Biousse V. Homonymous Hemianopia in Stroke. *J. Neuroophthalmol.* 2006;26:180.

4. Zhang X, Kedar S, Lynn MJ, Newman NJ, Biousse V. Natural history of homonymous hemianopia. *Neurology*. 2006;66:901–905.

5. Perez C, Chokron S. Rehabilitation of homonymous hemianopia: insight into blindsight. *Front. Integr. Neurosci.* 2014;8.

6. Peli E. Field expansion for homonymous hemianopia by optically induced peripheral exotropia. *Optom. Vis. Sci.* 2000;77:453–464.

7. Sahraie A, Smania N, Zihl J. Use of NeuroEyeCoach™ to Improve Eye Movement Efficacy in Patients with Homonymous Visual Field Loss. *BioMed Res. Int.* 2016;2016:5186461.

8. Weinberg J, Diller L, Gordon WA, Gerstman LJ, Lieberman A, Lakin P, Hodges G, Ezrachi O. Visual scanning training effect on reading-related tasks in acquired right brain damage. *Arch. Phys. Med. Rehabil.* 1977;58:479–486.

9. Pollock A, Hazelton C, Rowe FJ, Jonuscheit S, Kernohan A, Angilley J, Henderson CA, Langhorne P, Campbell P. Interventions for visual field defects in people with stroke. *Cochrane Database Syst. Rev.* 2019;5:CD008388.

10. Bergsma DP, Elshout JA, van den Berg AV. Segregation of Spontaneous and Training Induced Recovery from Visual Field Defects in Subacute Stroke Patients. *Front. Neurol.* 2017;8:681.

11. Cavanaugh MR, Huxlin KR. Visual discrimination training improves Humphrey perimetry in chronic cortically induced blindness. *Neurology*. 2017;88:1856–1864.

12. Cavanaugh MR, Zhang R, Melnick MD, Das A, Roberts M, Tadin D, Carrasco M, Huxlin KR. Visual recovery in cortical blindness is limited by high internal noise. *J. Vis.* 2015;15:9.

13. Chokron S, Perez C, Obadia M, Gaudry I, Laloum L, Gout O. From blindsight to sight: cognitive rehabilitation of visual field defects. *Restor. Neurol. Neurosci.* 2008;26:305–320.

14. Das A, Tadin D, Huxlin KR. Beyond blindsight: properties of visual relearning in cortically blind fields. *J. Neurosci.* 2014;34:11652–11664.

15. Huxlin KR, Martin T, Kelly K, Riley M, Friedman DI, Burgin WS, Hayhoe M. Perceptual relearning of complex visual motion after V1 damage in humans. *J. Neurosci.* 2009;29:3981–3991.

16. Melnick MD, Tadin D, Huxlin KR. Relearning to See in Cortical Blindness. *Neuroscientist*. 2016;22:199–212.

17. Raninen A, Vanni S, Hyvärinen L, Näsänen R. Temporal sensitivity in a hemianopic visual field can be improved by long-term training using flicker stimulation. *J. Neurol. Neurosurg. Psychiatry*. 2007;78:66–73.

18. Sahraie A, Macleod M-J, Trevethan CT, Robson SE, Olson JA, Callaghan P, Yip B. Improved detection following Neuro-Eye Therapy in patients with post-geniculate brain damage. *Exp. Brain Res.* 2010;206:25–34.

19. Saionz EL, Tadin D, Melnick MD, Huxlin KR. Functional preservation and enhanced capacity for visual restoration in subacute occipital stroke. *Brain*. 2020;143:1857–1872.

20. Trevethan CT, Urquhart J, Ward R, Gentleman D, Sahraie A. Evidence for perceptual learning with repeated stimulation after partial and total cortical blindness. *Adv. Cogn. Psychol.* 2012;8:29–37.

21. Vaina LM, Soloviev S, Calabro FJ, Buonanno F, Passingham R, Cowey A. Reorganization of retinotopic maps after occipital lobe infarction. *J. Cogn. Neurosci.* 2014;26:1266–1282.

22. Wang V, Saionz E, Cavanaugh M, Huxlin K. Natural progression of perimetric visual field defects after V1 stroke. *J. Vis.* 2017;17:51–52.

23. Saionz EL, Cavanaugh MR, Johnson BA, Harrington D, Aguirre GK, Huxlin KR. The natural history of homonymous hemianopia revisited [Internet]. 2022 [cited 2023 Feb 16];2022.10.06.22280668. Available from: https://www.medrxiv.org/content/10.1101/2022.10.06.22280668v1

24. Beatty R, Sadun A, Smith L, Vonsattel J, Richardson E. Direct demonstration of transsynaptic degeneration in the human visual system: a comparison of retrograde and anterograde changes. *J. Neurol. Neurosurg. Psychiatry*. 1982;45:143–146.

25. Bridge H, Jindahra P, Barbur J, Plant GT. Imaging Reveals Optic Tract Degeneration in Hemianopia. *Invest. Ophthalmol. Vis. Sci.* 2011;52:382–388.

26. Cowey A, Stoerig P, Perry VH. Transneuronal retrograde degeneration of retinal ganglion cells after damage to striate cortex in macaque monkeys: selective loss of P beta cells. *Neuroscience*. 1989;29:65–80.

27. Cowey A, Alexander I, Stoerig P. Transneuronal retrograde degeneration of retinal ganglion cells and optic tract in hemianopic monkeys and humans. *Brain*. 2011;134:2149–2157.

462 28. Herro A, Lam B. Retrograde degeneration of retinal ganglion cells in homonymous
463 hemianopsia. *Clin. Ophthalmol.* 2015;1057.

464 29. Jindahra P, Petrie A, Plant GT. Retrograde trans-synaptic retinal ganglion cell loss identified
465 by optical coherence tomography. *Brain*. 2009;132:628–634.

466 30. Jindahra P, Petrie A, Plant GT. The time course of retrograde trans-synaptic degeneration
467 following occipital lobe damage in humans. *Brain*. 2012;135:534–541.

468 31. Park H-YL, Park YG, Cho A-H, Park CK. Transneuronal Retrograde Degeneration of the
469 Retinal Ganglion Cells in Patients with Cerebral Infarction. *Ophthalmology*.
470 2013;120:1292–1299.

471 32. Meier PG, Maeder P, Kardon RH, Borruat F-X. Homonymous Ganglion Cell Layer Thinning
472 After Isolated Occipital Lesion: Macular OCT Demonstrates Transsynaptic Retrograde
473 Retinal Degeneration. *J. Neuroophthalmol.* 2014;1.

474 33. Millington RS, Yasuda CL, Jindahra P, Jenkinson M, Barbur JL, Kennard C, Cendes F, Plant GT,
475 Bridge H. Quantifying the pattern of optic tract degeneration in human hemianopia. *J.*
476 *Neurol. Neurosurg. Psychiatry*. 2014;85:379–386.

477 34. Yamashita T, Miki A, Goto K, Araki S, Takizawa G, Ieki Y, Kiryu J, Tabuchi A, Iguchi Y, Kimura
478 K, et al. Retinal Ganglion Cell Atrophy in Homonymous Hemianopia due to Acquired
479 Occipital Lesions Observed Using Cirrus High-Definition-OCT. *J. Ophthalmol.* 2016;2016:1–
480 9.

481 35. Fahrenthold BK, Cavanaugh MR, Jang S, Murphy AJ, Ajina S, Bridge H, Huxlin KR. Optic Tract
482 Shrinkage Limits Visual Restoration After Occipital Stroke. *Stroke*. 2021;52:3642–3650.

483 36. Schneider CL, Prentiss EK, Busza A, Matmati K, Matmati N, Williams ZR, Sahin B, Mahon BZ.
484 Survival of retinal ganglion cells after damage to the occipital lobe in humans is activity
485 dependent. *Proc R Soc B Biol Sci*. 2019;286:9.

486 37. Goto K, Miki A, Yamashita T, Araki S, Takizawa G, Nakagawa M, Ieki Y, Kiryu J. Sectoral
487 analysis of the retinal nerve fiber layer thinning and its association with visual field loss in
488 homonymous hemianopia caused by post-geniculate lesions using spectral-domain optical
489 coherence tomography. *Graefes Arch. Clin. Exp. Ophthalmol.* 2016;254:745–756.

490 38. Keller J, Sánchez-Dalmau BF, Villoslada P. Lesions in the Posterior Visual Pathway Promote
491 Trans-Synaptic Degeneration of Retinal Ganglion Cells. *PLoS ONE*. 2014;9:e97444.

492 39. Mehta JS, Plant GT. Optical Coherence Tomography (OCT) Findings in Congenital/Long-
493 Standing Homonymous Hemianopia. *Am. J. Ophthalmol.* 2005;140:727–729.

40. Mitchell JR, Oliveira C, Tsiouris AJ, Dinkin MJ. Corresponding Ganglion Cell Atrophy in Patients With Postgeniculate Homonymous Visual Field Loss: *J. Neuroophthalmol.* 2015;35:353–359.

41. Porrello G, Falsini B. Retinal ganglion cell dysfunction in humans following post-geniculate lesions: specific spatio–temporal losses revealed by pattern ERG. *Vision Res.* 1999;39:1739–1748.

42. Shin H-Y, Park H-YL, Choi J-A, Park CK. Macular ganglion cell–inner plexiform layer thinning in patients with visual field defect that respects the vertical meridian. *Graefes Arch. Clin. Exp. Ophthalmol.* 2014;252:1501–1507.

43. Simmen CF, Fierz FC, Michels L, Aldusary N, Landau K, Piccirelli M, Traber GL. Lateral Geniculate Nucleus Volume Determined on MRI Correlates With Corresponding Ganglion Cell Layer Loss in Acquired Human Postgeniculate Lesions. *Invest. Ophthalmol. Vis. Sci.* 2022;63:18.

44. Yamashita T, Miki A, Goto K, Araki S, Takizawa G, Ieki Y, Kiryu J, Tabuchi A, Iguchi Y, Kimura K, et al. Evaluation of Significance Maps and the Analysis of the Longitudinal Time Course of the Macular Ganglion Cell Complex Thicknesses in Acquired Occipital Homonymous Hemianopia Using Spectral-domain Optical Coherence Tomography. *Neuro-Ophthalmol.* 44:236–245.

45. Zangerl B, Whatham A, Kim J, Choi A, Assaad NN, Hennessy MP, Kalloniatis M. Reconciling visual field defects and retinal nerve fibre layer asymmetric patterns in retrograde degeneration: an extended case series: Retinal nerve fibre layer defects in retrograde degeneration. *Clin. Exp. Optom.* 2017;100:214–226.

46. Saionz EL, Busza A, Huxlin KR. Chapter 25 - Rehabilitation of visual perception in cortical blindness [Internet]. In: Quartarone A, Ghilardi MF, Boller F, editors. Handbook of Clinical Neurology. Elsevier; 2022 [cited 2023 Nov 15]. p. 357–373.Available from: https://www.sciencedirect.com/science/article/pii/B9780128194102000308

47. Brown CE, Aminoltejari K, Erb H, Winship IR, Murphy TH. In Vivo Voltage-Sensitive Dye Imaging in Adult Mice Reveals That Somatosensory Maps Lost to Stroke Are Replaced over Weeks by New Structural and Functional Circuits with Prolonged Modes of Activation within Both the Peri-Infarct Zone and Distant Sites. *J. Neurosci.* 2009;29:1719–1734.

48. Brown CE, Li P, Boyd JD, Delaney KR, Murphy TH. Extensive Turnover of Dendritic Spines and Vascular Remodeling in Cortical Tissues Recovering from Stroke. *J. Neurosci.* 2007;27:4101–4109.

49. Harrison TC, Silasi G, Boyd JD, Murphy TH. Displacement of Sensory Maps and Disorganization of Motor Cortex After Targeted Stroke in Mice. *Stroke*. 2013;44:2300–2306.

50. Cavanaugh MR, Blanchard LM, McDermott M, Lam BL, Tamhankar M, Feldon SE. Efficacy of Visual Retraining in the Hemianopic Field after Stroke: Results of a Randomized Clinical Trial. *Ophthalmology*. 2021;128:1091–1101.

51. Barbot A, Das A, Melnick MD, Cavanaugh MR, Merriam EP, Heeger DJ, Huxlin KR. Spared perilesional V1 activity underlies training-induced recovery of luminance detection sensitivity in cortically-blind patients. *Nat. Commun.* 2021;12:6102.

52. Jansonius NM, Schiefer J, Nevalainen J, Paetzold J, Schiefer U. A mathematical model for describing the retinal nerve fiber bundle trajectories in the human eye: Average course, variability, and influence of refraction, optic disc size and optic disc position. *Exp. Eye Res.* 2012;105:70–78.

53. Cowey A, Alexander I, Stoerig P. Transneuronal retrograde degeneration of retinal ganglion cells and optic tract in hemianopic monkeys and humans. *Brain*. 2011;134:2149–2157.

54. Cowey A. Atrophy of Retinal Ganglion Cells after Removal of Striate Cortex in a Rhesus Monkey. *Perception*. 1974;3:257–260.

55. Johnson H, Cowey A. Transneuronal retrograde degeneration of retinal ganglion cells following restricted lesions of striate cortex in the monkey. *Exp. Brain Res.* 2000;132:269–275.

56. Buren JMV. Trans-synaptic retrograde degeneration in the visual system of primates. *J. Neurol. Neurosurg. Psychiatry*. 1963;26:402–409.

57. Davis BM, Guo L, Ravindran N, Shamsher E, Baekelandt V, Mitchell H, Bharath AA, De Groef L, Cordeiro MF. Dynamic changes in cell size and corresponding cell fate after optic nerve injury. *Sci. Rep.* 2020;10:21683.

58. Miettinen TP, Björklund M. Mitochondrial Function and Cell Size: An Allometric Relationship. *Trends Cell Biol.* 2017;27:393–402.

59. Zhang X, Francis BA, Dastiridou A, Chopra V, Tan O, Varma R, Greenfield DS, Schuman JS, Huang D. Longitudinal and Cross-Sectional Analyses of Age Effects on Retinal Nerve Fiber Layer and Ganglion Cell Complex Thickness by Fourier-Domain OCT. *Transl. Vis. Sci. Technol.* 2016;5:1.

60. Saenz M, Fine I. Topographic Organization of V1 Projections through the Corpus Callosum in Humans. *NeuroImage*. 2010;52:1224–1229.

61. El-Danaf RN, Huberman AD. Characteristic Patterns of Dendritic Remodeling in Early-Stage Glaucoma: Evidence from Genetically Identified Retinal Ganglion Cell Types. *J. Neurosci.* 2015;35:2329–2343.

563 62. Amato R, Catalani E, Dal Monte M, Cammalleri M, Cervia D, Casini G. Morpho-functional
564 analysis of the early changes induced in retinal ganglion cells by the onset of diabetic
565 retinopathy: The effects of a neuroprotective strategy. *Pharmacol. Res.* 2022;185:106516.

566 63. Vecino E, Rodriguez FD, Ruzafa N, Pereiro X, Sharma SC. Glia–neuron interactions in the
567 mammalian retina. *Prog. Retin. Eye Res.* 2016;51:1–40.

568

569

570 **Figure Legends**

571

572 **Figure 1. A:** Computation of LI for the GCL-IPL using the nasal (N) and temporal (T) sector GCL-
573 IPL (GI) thickness values of both eyes, excluding superior (S) and inferior (I) sectors since they
574 overlapped the vertical meridian. **B:** Plot comparing GCL-IPL thicknesses in the affected or
575 unaffected hemiretinas (*paired t-test, CI_{95} =5.212 to 10.60, t_{42} =5.921, p = <0.0001*). **C:** Plot of
576 $LI_{GCL-IPL}$ against time since stroke (*linear regression, R^2=0.2703, CI_{95}(y-intercept)=0.018 to 0.057,*
577 *p=0.0004)*.

578

579 **Figure 2. A:** Computation of LI using RNFL thickness values (R) from superior (S) and inferior (I)
580 peripapillary regions comprised of uncrossed fibers, and nasal (N) peripapillary regions
581 comprised of crossed fibers representing intact or blind hemifields. **B:** Plot comparing affected
582 peripapillary RNFL segments carrying RGC axons representing the visual field defect to
583 unaffected carrying predominantly intact field fibers (*paired t-test, CI_{95} =1.046 to 5.450, t_{42} =*
584 *2.977, p = 0.0048*). **C:** Plot of LI_{RNFL} against time since stroke (*linear regression, R^2=0.2293, CI_{95}=-*
585 *0.0004 to 0.0217, p=0.0012)*.

586

587 **Figure 3. A:** Plot of pre- and post-training OU MD in BF-trained participants (*paired t-test, CI_{95}*
588 *=0.098 to 1.2, t_{18} = 2.473, p = 0.023, mean of differences = 0.65±1.15)*. **B:** OU ST_{BF} pre- and post-
589 training following BF training *(paired t-test, CI_{95} =0.177 to 2.258, t_{18} = 2.458, p = 0.024, mean of*
590 *differences = 1.22±2.16).* **C:** Linear regression of MD against ST_{BF} pre-training: *R^2=0.9365, CI_{95}(y-*
591 *intercept)=-18.28 to -16.82;* post-BF training: *p <0.0001; R^2=0.9526, CI_{95}(y-intercept)=-18.21 to -*

592 *16.84, p <0.0001*. **D:** Plot of pre- and post-training OU MD in IF-trained participants (*paired t-*

593 *test, CI_{95} =-0.3284 to 0.6284, t_{18} = 0.6587, p = 0.5184, mean of differences = 1.5±0.9926).* **E:** OU

594 ST_{BF} pre- and post-training following IF training (*paired t-test, CI_{95} =-0.1917 to 0.8655, t_{18} =*

595 *1.339, p = 0.1972, mean of differences = 0.3369±1.097*). **F:** Linear regression of MD against ST_{BF}

596 pre-training: *R^2=0.963, CI_{95}(y-intercept)=-17.04 to -15.87; post-IF training: p <0.0001; R^2=0.9481,*

597 *CI_{95}(y-intercept)=-17.67 to -16.08, p <0.0001*). ns: not statistically significant.

598

599 **Figure 4. A:** Plot of $LI_{GCL-IPL}$ pre- to post-training for all participants (*paired t-test, CI_{95} =0.005 to*

600 *0.019, t_{42} = 3.424, p = 0.001*). **B:** Plot of LI_{RNFL} pre- to post-training of all participants (*paired t-*

601 *test, CI_{95} =-0.0015 to 0.01251, t_{42} = 1.572, p = 0.1234*). ns: not statistically significant.

602

603 **Figure 5. A:** Plot of $LI_{GCL-IPL}$ pre- to post-training of participants who trained in their IF (*paired t-*

604 *test, CI_{95} =0.003 to 0.025, t_{22} = 2.837, p = 0.0096*). **B:** Plot of $LI_{GCL-IPL}$ pre- to post-training of

605 participants who trained in their BF (*paired t-test, CI_{95} = -0.0008 to 0.0199, t_{19} = 1.916, p = 0.07*).

606 **C:** Comparisons of unaffected and affected hemiretina GCL-IPL thicknesses, before and after

607 training in the IF (*unaffected pre- vs post-training: paired t-test, CI_{95}= -1.017 to 0.4516, p =*

608 *0.4332; affected pre- vs post-training: paired t-test, CI_{95} = -3.233 to -1.093, p = 0.0004).* **D:**

609 Comparison of unaffected and affected hemiretina GCL-IPL thicknesses, before and after BF

610 training (*unaffected pre- vs post-training: paired t-test, CI_{95} = -0.8943 to 0.4443, p = 0.4902;*

611 *affected pre- vs post-training: paired t-test, CI_{95} = -2.691 to -0.0843, p = 0.04).* **E:** Comparison of

612 change in GCL-IPL thickness from pre- to post-training in IF or BF-trained participants

613 (*unaffected vs affected hemiretina in IF-trained subjects, paired t-test, CI_{95}=0.2063 to 3.555,*

p=0.009; *unaffected vs affected hemiretina in BF-trained subjects, CI_{95}=-2.601 to 0.2762, p=0.1071*; *unaffected vs unaffected of both training groups, unpaired t-test, CI_{95}=-0.9176 to 1.033, p=0.9056*; *affected vs affected of both training groups, unpaired t-test, CI_{95}=-0.8438 to 2.395, p=0.3391*). A: Affected, UA: Unaffected, ns: not statistically significant.

Figure 6. A: Plot of LI_{RNFL} pre- to post-training of participants who trained in their IF (*paired t-test, CI_{95} =-0.003 to 0.0123, t_{22} = 0.7322, p = 0.4718*). **B:** Plot of LI_{RNFL} pre- to post-training of participants who trained in their BF (*paired t-test, CI_{95} = -0.0036 to 0.0197, t_{19} = 1.446, p = 0.1645*). **C:** Comparison of unaffected and affected RNFL thicknesses, before and after IF training (*unaffected pre- vs post-training: paired t-test, CI_{95} = -1.860 to 0.8163, p = 0.4274; affected pre- vs post-training: paired t-test, CI_{95} = -2.796 to 0.7962, p = 0.2606).* **D:** Comparison of unaffected and affected RNFL thicknesses, before and after BF training (*unaffected pre- vs post-training: paired t-test, CI_{95} = -1.714 to 2.414, p = 0.7266; affected pre- vs post-training: paired t-test, CI_{95} = -2.862 to 0.3951, p = 0.1294).* **E:** Comparison of change in RNFL thickness from pre- to post-training in IF or BF-trained participants (*unaffected vs affected in IF-trained subjects: paired t-test, CI_{95}=-2.096 to 1.139, p=0.546*; *unaffected vs affected in BF-trained subjects: paired t-test, CI_{95}=-3.627 to 0.4601, p=0.1213*; *unaffected vs unaffected of both training groups: unpaired t-test, CI_{95}=-1.451 to 3.195, p=0.4529*; *affected vs affected of both training groups: unpaired t-test, CI_{95}=-2.614 to 2.148, p=0.8441*). A: Affected, UA: Unaffected, ns: not statistically significant.

635 **Figure 7. A:** Plot of change in ST_{BF} against $LI_{GCL\text{-}IPL}$ of participants trained in their IF (*linear*

636 *regression, R^2=0.0307, CI_{95}(y-intercept)=-0.3997 to 0.8511, p=0.4727).* **B:** Plot of changes in ST_{BF}

637 and LI_{RNFL} in IF-trained participants (*linear regression, R^2=0.001, CI_{95}(y-intercept)=-0.3497 to*

638 *0.766, p=0.8857*). **C:** Plot of change in ST_{BF} against $LI_{GCL\text{-}IPL}$ of participants trained in their BF

639 (*linear regression, R^2=0.2170, CI_{95}(y-intercept)=0.6239 to 2.723, p=0.04).* **D:** Plot of changes in

640 ST_{BF} and LI_{RNFL} in participants training in the BF (*linear regression, R^2=0.0196, CI_{95}(y-*

641 *intercept)=0.0093 to 2.241, p=0.5674*).

642

643

644 **Table 1. Participant demographics**. m: male, f: female, R: right, L: left.

Subject code	Sex	Age range (years)	Time since stroke (months)	Affected visual hemifield	Training Group
CB1	m	46-50	32	R	Intact
CB2	f	46-50	13	R	Intact
CB3	m	70-75	20	L	Intact
CB4	m	60-65	61	L	Intact
CB5	m	60-65	43	L	Intact
CB6	m	55-60	105	R	Intact
CB7	f	70-75	338	L	Intact
CB8	m	70-75	10	L	Intact
CB9	m	66-70	6	R	Intact
CB10	m	70-75	4	L	Intact
CB11	m	70-75	58	L	Intact
CB12	f	66-70	16	R	Intact
CB13	f	50-55	24	L	Intact
CB14	m	60-65	130	L	Intact
CB15	m	56-60	13	L	Intact
CB16	m	46-50	63	L	Intact
CB17	m	60-65	8	L	Intact
CB18	f	46-50	15	R	Intact
CB19	m	60-65	20	R	Intact
CB20	m	40-45	5	R	Intact
CB21	m	66-70	3	R	Intact
CB22	m	56-60	4	R	Intact
CB23	m	70-75	6	L	Intact
CB24	m	66-70	60	L	Blind
CB25	f	50-55	38	R	Blind
CB26	f	50-55	18	L	Blind
CB27	m	40-45	15	R	Blind
CB28	m	50-55	373	R	Blind
CB29	m	60-65	5	R	Blind
CB30	m	70-75	47	R	Blind
CB31	m	56-60	8	L	Blind
CB32	m	60-65	47	L	Blind
CB33	m	40-45	11	R	Blind
CB34	m	56-60	4	L	Blind
CB35	f	40-45	10	R	Blind
CB36	m	66-70	105	L	Blind
CB37	m	66-70	36	R	Blind
CB38	m	30-35	5	R	Blind
CB39	f	46-50	5	L	Blind
CB40	f	60-65	3	L	Blind
CB41	m	46-50	14	R	Blind
CB42	m	66-70	3	L	Blind
CB43	m	70-75	6	L	Blind

645
646

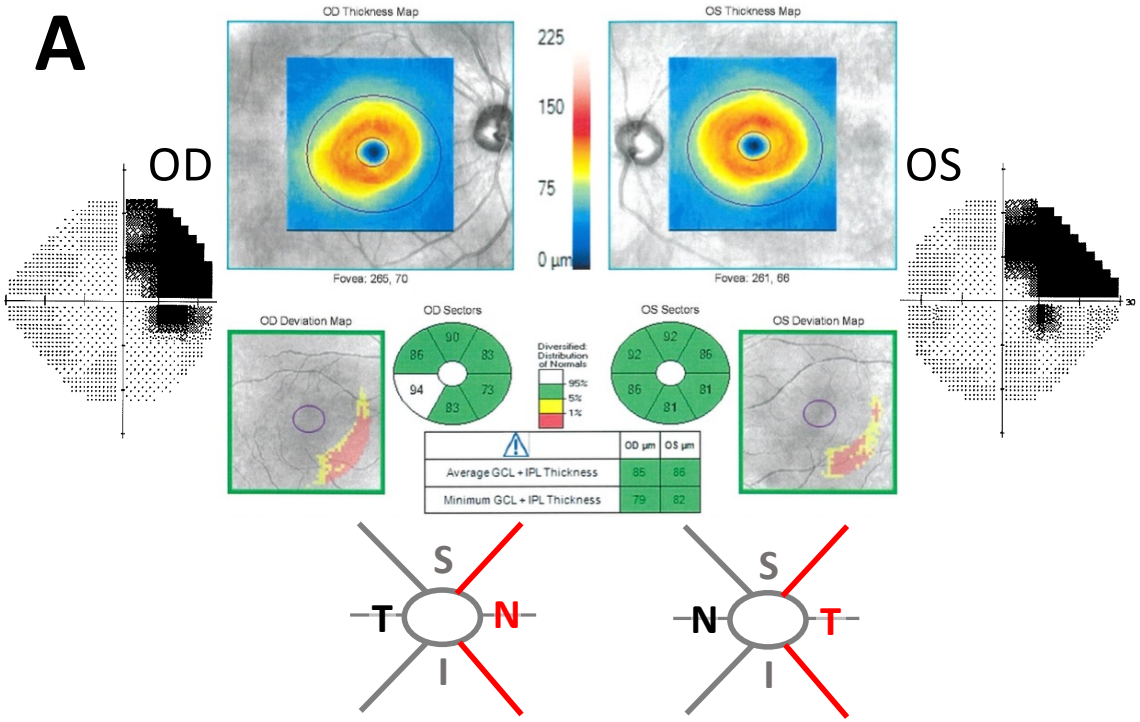

$$LI_{GCL\text{-}IPL} = \frac{[(GI_{T\_OD}+GI_{N\_OS})/2)-(GI_{N\_OD}+GI_{T\_OS})/2)]}{[(GI_{T\_OD}+GI_{N\_OS})/2)+(GI_{N\_OD}+GI_{T\_OS})/2)]}$$

(Right deficit)

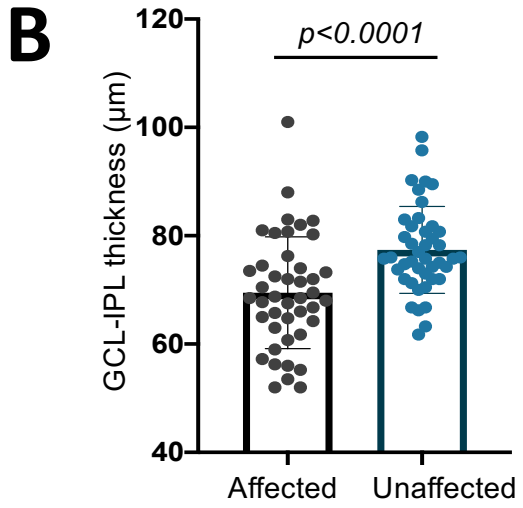

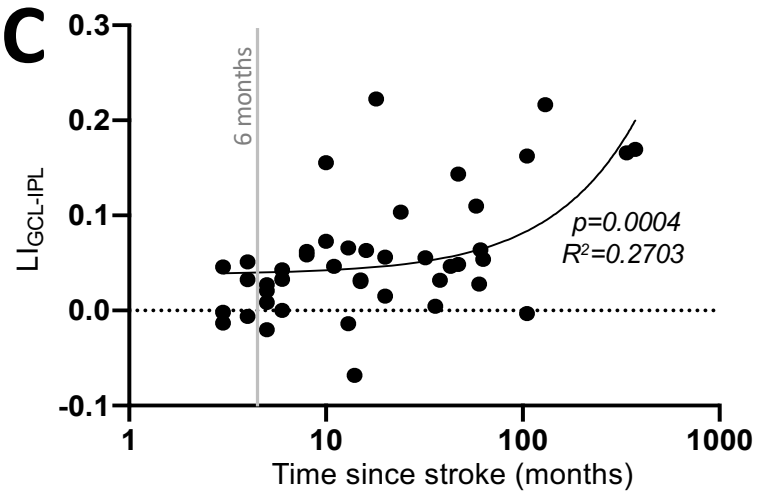

Figure 2

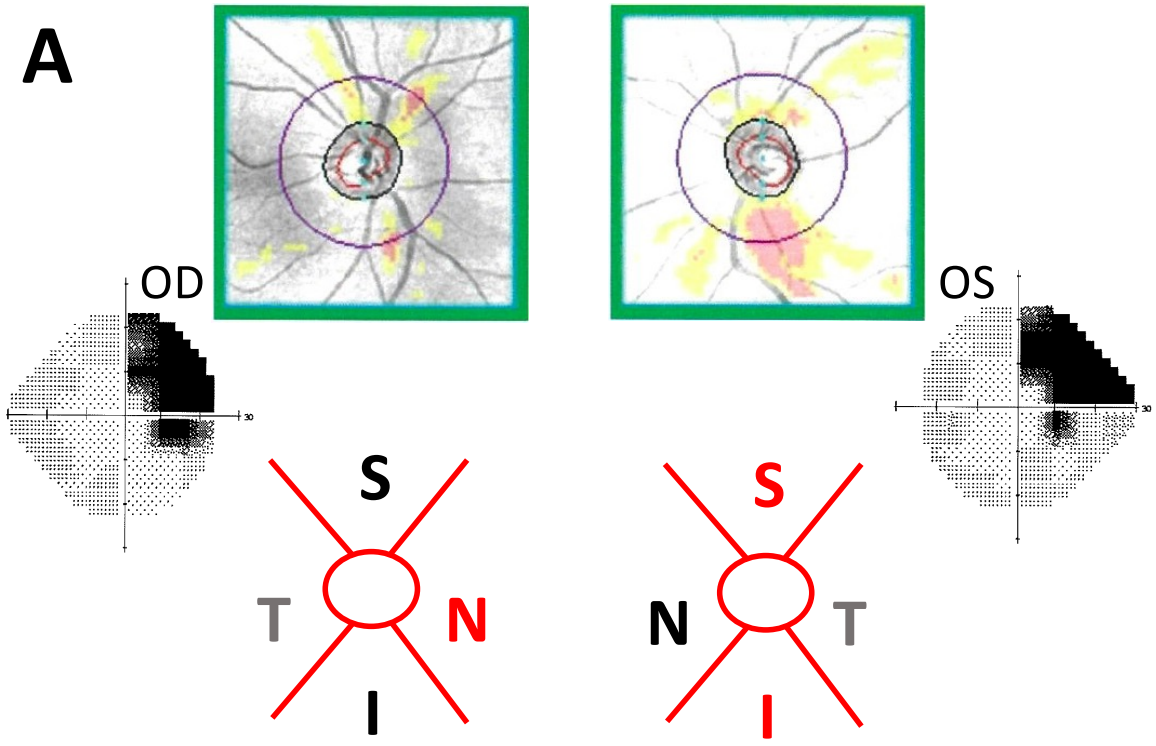

$$LI_{RNFL} = \frac{((R_{S\_OD}+R_{I\_OD}+R_{N\_OS})/3)-(R_{S\_OS}+R_{I\_OS}+R_{N\_OD})/3))}{((R_{S\_OD}+R_{I\_OD}+R_{N\_OS})/3)+(R_{S\_OS}+R_{I\_OS}+R_{N\_OD})/3))}$$

(Right deficit)

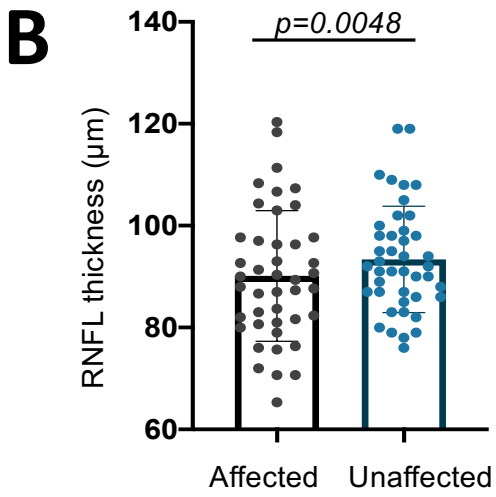

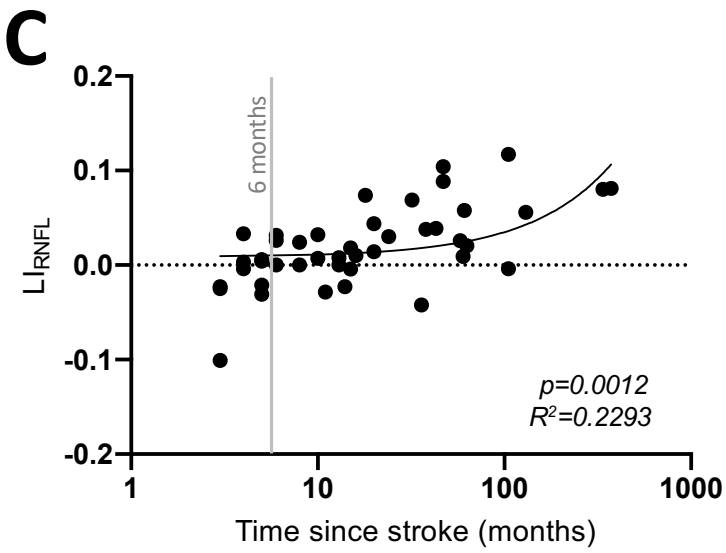

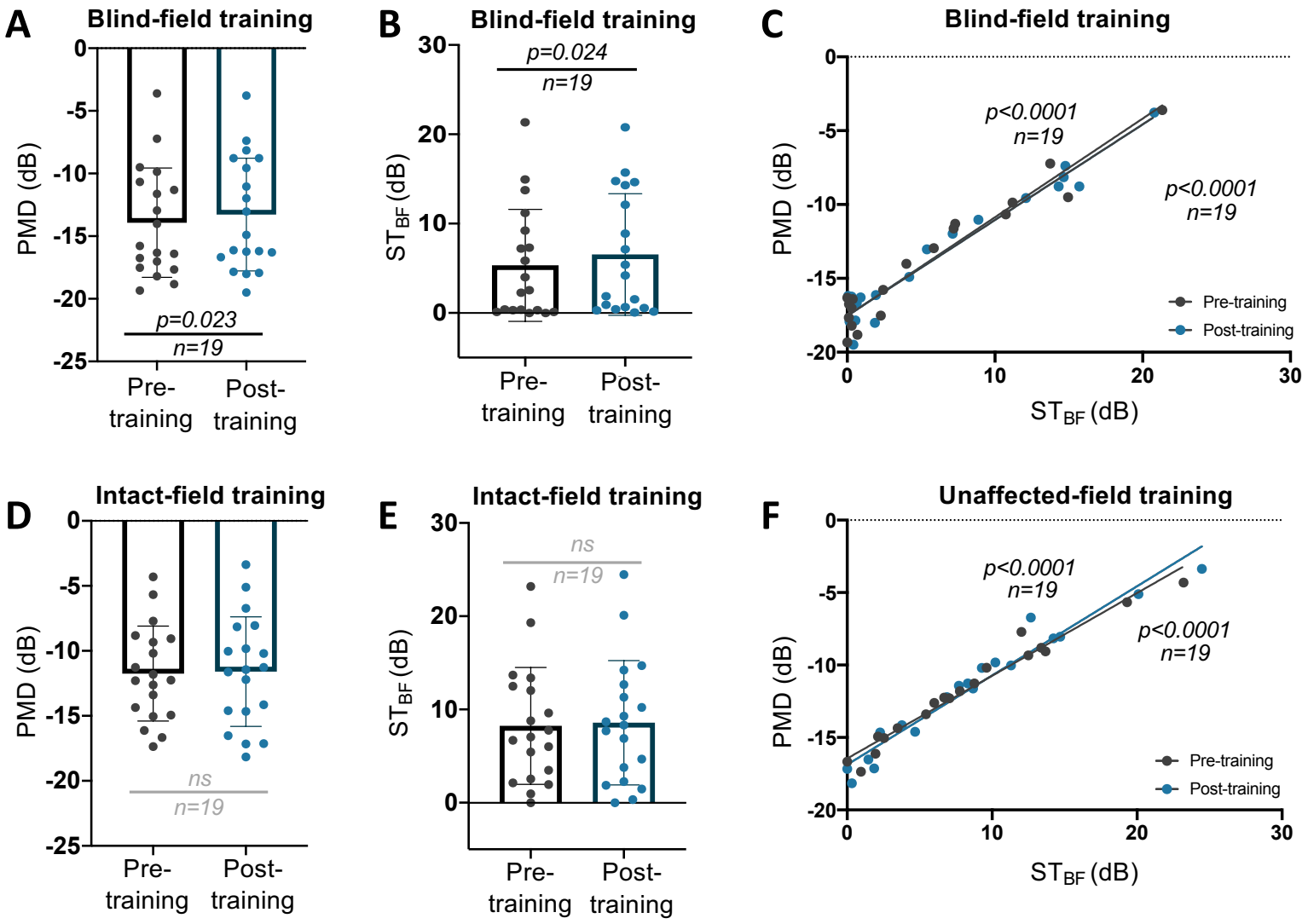
A
Blind-field training
PMD (dB)
0
-5
-10
-15
-20
-25
p=0.023
n=19
Pre-training
Post-training
B
Blind-field training
ST_BF (dB)
30
20
10
0
p=0.024
n=19
Pre-training
Post-training
C
Blind-field training
PMD (dB)
ST_BF (dB)
p<0.0001
n=19
p<0.0001
n=19
Pre-training
Post-training
D
Intact-field training
PMD (dB)
ns
n=19
Pre-training
Post-training
E
Intact-field training
ST_BF (dB)
ns
n=19
Pre-training
Post-training
F
Unaffected-field training
PMD (dB)
ST_BF (dB)
p<0.0001
n=19
p<0.0001
n=19
Pre-training
Post-training

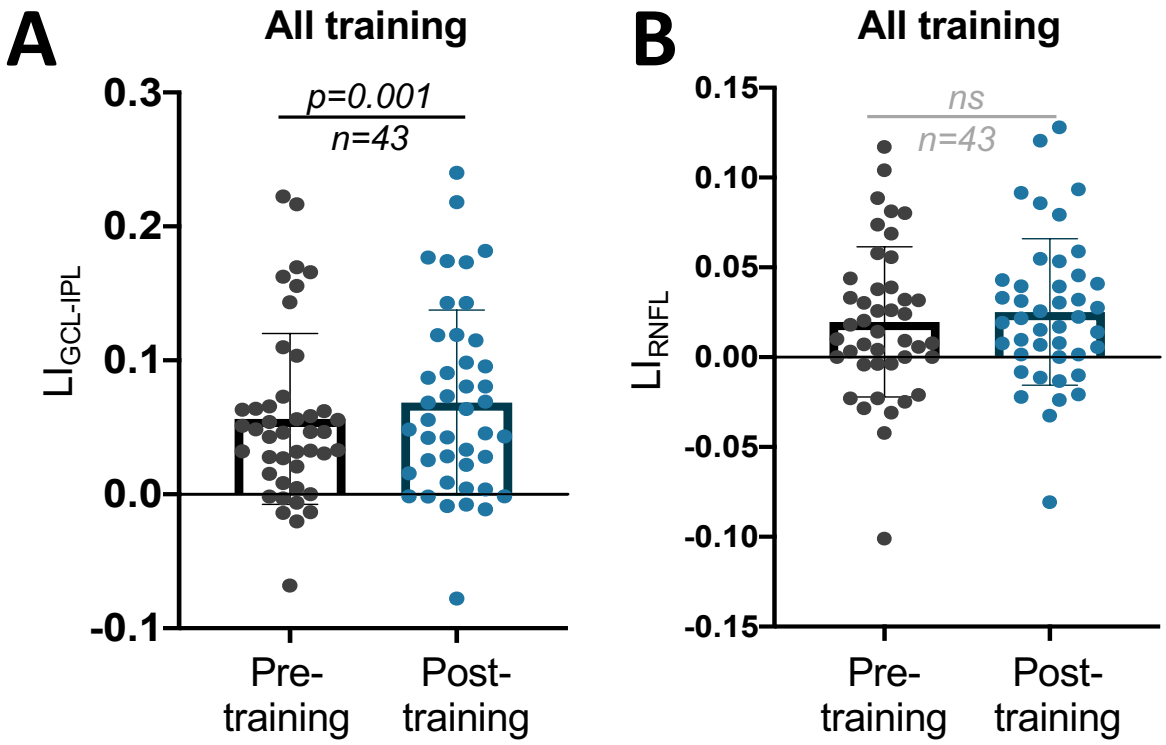
A
All training
p=0.001
n=43
0.3
0.2
0.1
0.0
-0.1
LI GCL-IPL
Pre-training
Post-training
B
All training
ns
n=43
0.15
0.10
0.05
0.00
-0.05
-0.10
-0.15
LI RNFL
Pre-training
Post-training

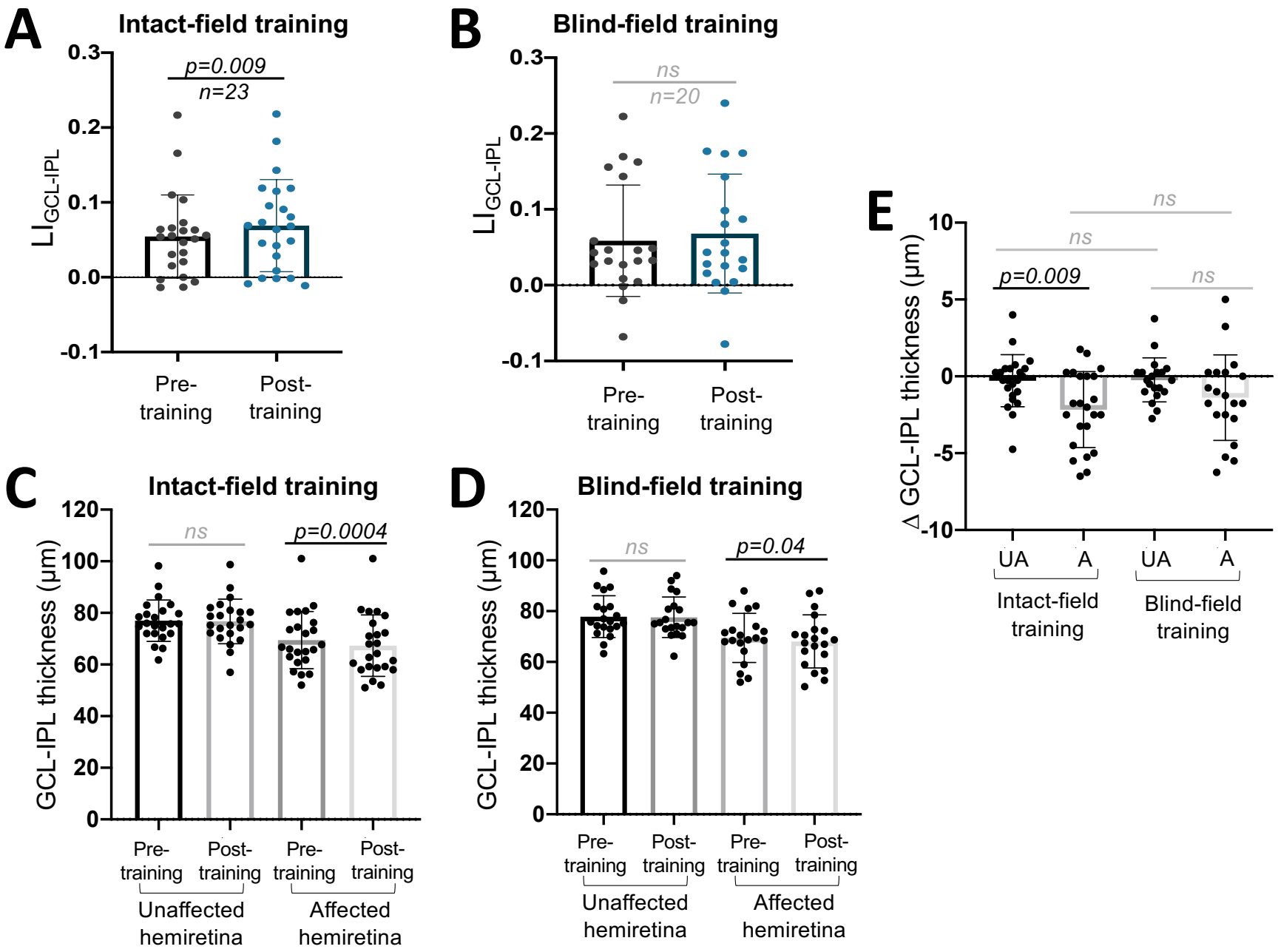
A
Intact-field training
p=0.009
n=23
LI GCL-IPL
0.3
0.2
0.1
0.0
-0.1
Pre-training
Post-training
B
Blind-field training
ns
n=20
LI GCL-IPL
0.3
0.2
0.1
0.0
-0.1
Pre-training
Post-training
C
Intact-field training
GCL-IPL thickness (µm)
ns
p=0.0004
120
100
80
60
40
20
0
Pre-training
Post-training
Pre-training
Post-training
Unaffected hemiretina
Affected hemiretina
D
Blind-field training
GCL-IPL thickness (µm)
ns
p=0.04
120
100
80
60
40
20
0
Pre-training
Post-training
Pre-training
Post-training
Unaffected hemiretina
Affected hemiretina
E
Δ GCL-IPL thickness (µm)
ns
ns
ns
p=0.009
10
5
0
-5
-10
UA
A
UA
A
Intact-field training
Blind-field training

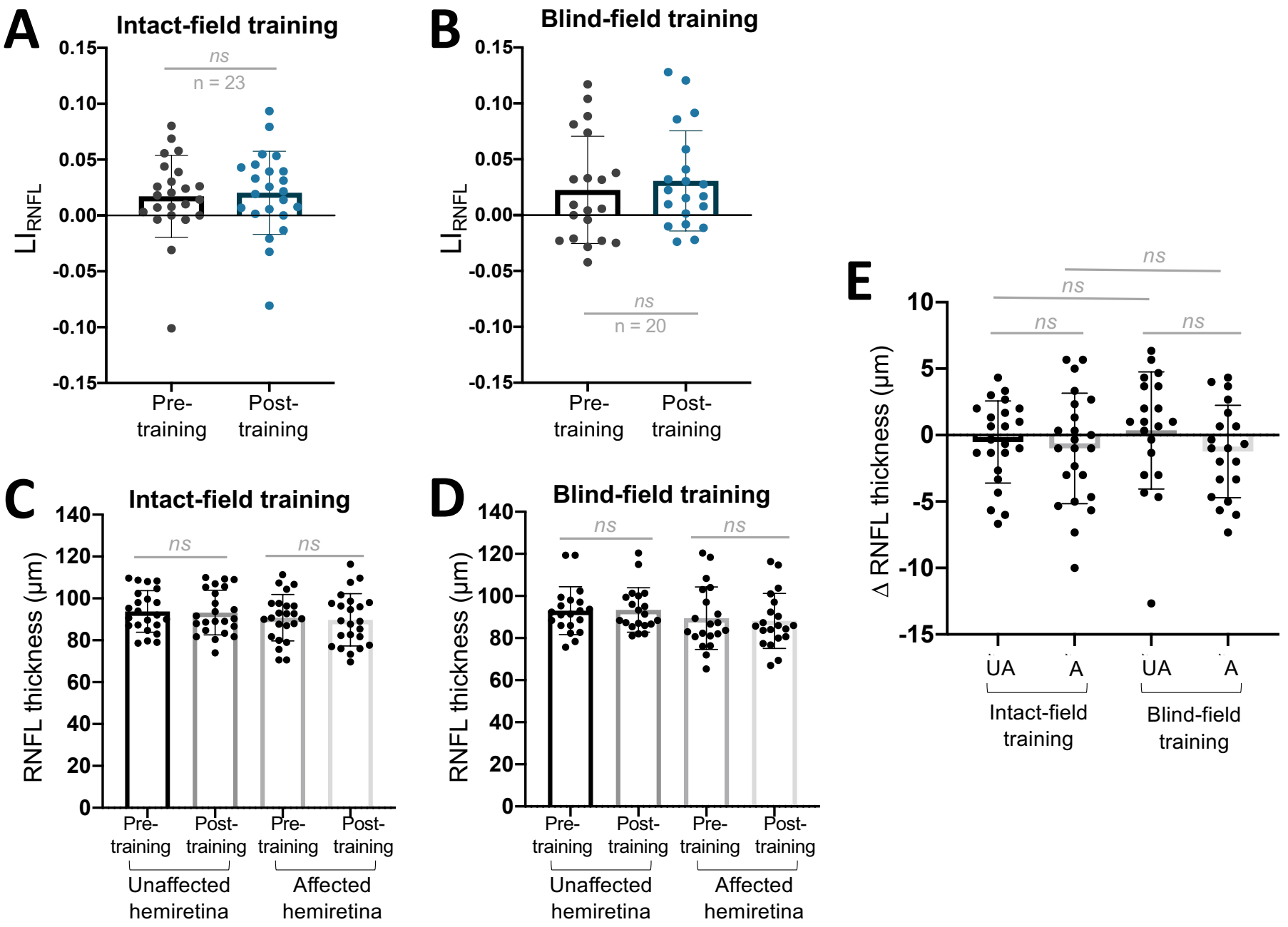
A
Intact-field training
ns
n = 23
LI RNFL
0.15
0.10
0.05
0.00
-0.05
-0.10
-0.15
Pre-training
Post-training
B
Blind-field training
ns
n = 20
C
Intact-field training
RNFL thickness (µm)
140
120
100
80
60
40
20
0
Unaffected hemiretina
Affected hemiretina
D
Blind-field training
E
Δ RNFL thickness (µm)
10
5
0
-5
-10
-15
UA
A
Intact-field training
Blind-field training

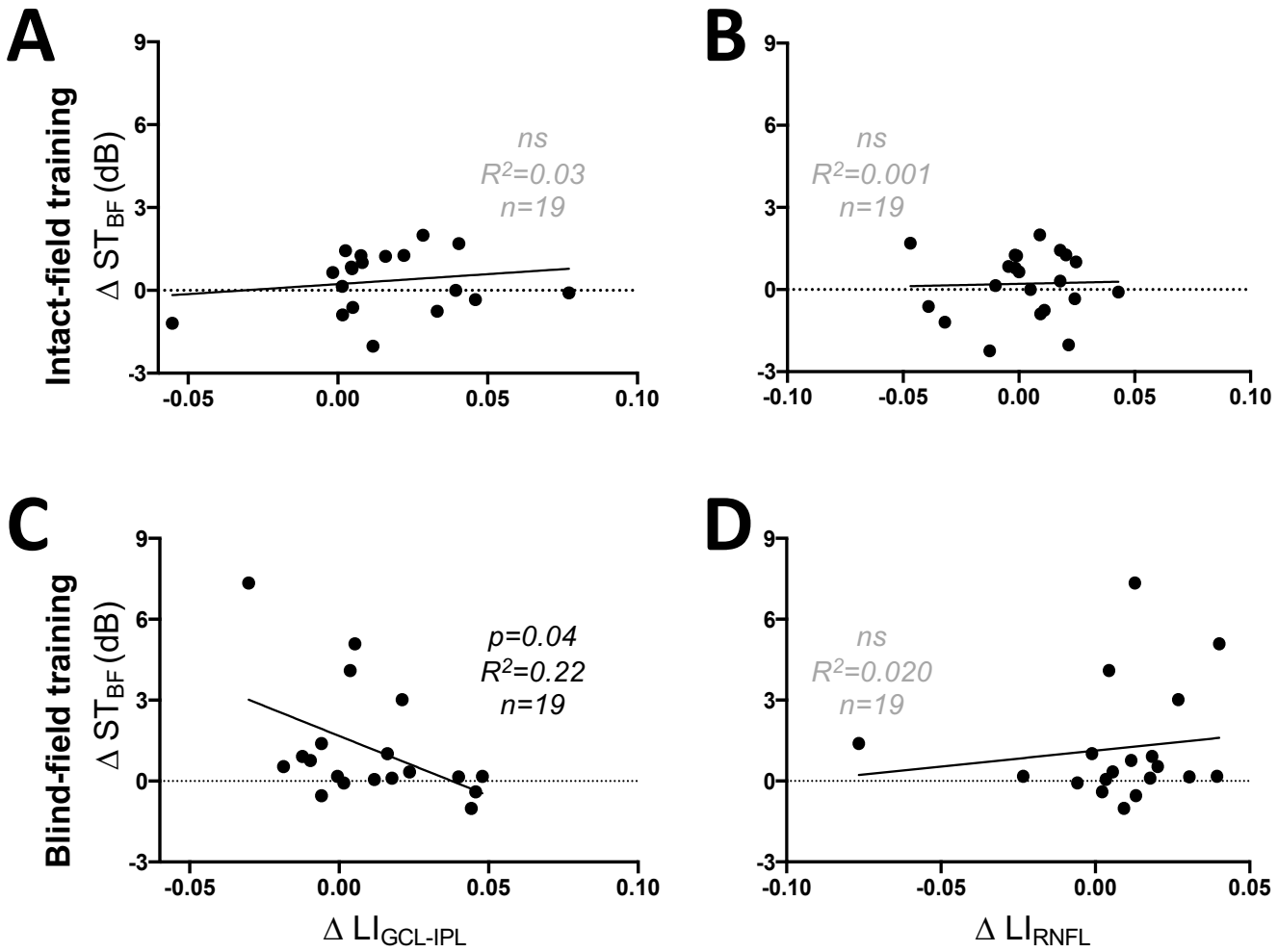
A
B
C
D
Intact-field training
Blind-field training
Δ ST_BF (dB)
ns
R²=0.03
n=19
ns
R²=0.001
n=19
p=0.04
R²=0.22
n=19
ns
R²=0.020
n=19
Δ LI_GCL-IPL
Δ LI_RNFL
9
6
3
0
-3
-0.10
-0.05
0.00
0.05
0.10